

## Comprehensive Calculations of the $(\pi^+, K^+)$ Reaction on $^{12}\text{C}$

Dean Halderson, Yizhang Mo,<sup>(a)</sup> and Pingzhi Ning<sup>(b)</sup>

*Physics Department, Western Michigan University, Kalamazoo, Michigan 49008*

(Received 9 June 1986)

The results of comprehensive distorted-wave impulse-approximation calculations are presented for the reaction  $^{12}\text{C}(\pi^+, K^+)^{12}\text{C}$  and compared to recent experimental data. The calculation includes scattering from bound states and resonances plus quasifree scattering in one consistent formalism. The features of the data are reproduced by the calculation, and these features are identified with underlying shell-model configurations.

PACS numbers: 25.80.Hp, 21.80.+a

The  $(\pi^+, K^+)$  reaction has been suggested as an excellent means of obtaining hypernuclear structure information which is complementary to that obtained by  $(K^-, \pi^-)$ .<sup>1</sup> Whereas the elementary reaction  $K^- + n \rightarrow \pi^- + \Lambda$  possesses a magic momentum at which no momentum is transferred to the lambda, the reaction  $\pi^+ + n \rightarrow K^+ + \Lambda$  transfers 300–350 MeV/c of momentum at typical  $\pi^+$  energies. The  $(\pi^+, K^+)$  reaction will, therefore, preferentially excite high spin states at  $0^\circ$ , while the  $(K^-, \pi^-)$  reaction preferentially excites  $0^+$  states at  $0^\circ$  on nuclei with  $0^+$  ground states. By combining the results of both reactions, one can obtain a more complete spectrum of natural-parity states and add to the knowledge of the  $\Lambda N$  interaction.

The first observation of  $\Lambda$ -hypernuclear structure via  $(\pi^+, K^+)$  was reported in a recent Letter.<sup>2</sup> Pions with momentum 1054 MeV/c were incident on a  $^{12}\text{C}$  target producing  $^{12}\text{C}$ . The resulting spectrum showed a sharp feature for the  $^{12}\text{C}$  ground state, a sharp feature near  $\Lambda$  threshold, and a large quasifree region. The presence of a large quasifree region has generally made identification of states and extraction of strength more difficult. Theoretical guidance is limited because

hypernuclear states are generally calculated in a shell model,<sup>3</sup> while the quasifree scattering is generally calculated in a Fermi-gas model.<sup>4</sup> Efforts to combine the processes in one calculation have normally required abandoning the sophistication of the shell model, e.g., realistic interactions and configurations free of center-of-mass excitations. However, in this Letter the results of a calculation for  $^{12}\text{C}(\pi^+, K^+)^{12}\text{C}$  are presented in which bound states, resonances, and quasifree scattering are all treated in one consistent formalism, while retaining the virtues of the shell model. The features of the experimental spectrum are then interpreted in terms of the shell-model configurations.

The formalism employed in this Letter is that of the recoil-corrected continuum shell model (RCCSM).<sup>5,6</sup> The RCCSM generates hyperon wave functions in terms of internal coordinates by solving the translationally invariant Hamiltonian

$$H = H_{\text{core}} + p_\Lambda^2/2m + \sum_{i=1}^A v_{\Lambda N_i} - T_{\text{c.m.}}$$

To accommodate this coordinate system the distorted-wave cross section is given by<sup>6</sup>

$$d\sigma/d\Omega = [j_i]^{-1} \sum_{M_i M_f} (2\pi/\hbar c)^4 (k_f/k_i) (\omega_\pi \omega_A \omega_K \omega_B / S) |T_{ba}|^2, \quad (1)$$

where

$$T_{ba} = \sum_i \int \chi_f^{(-)*} [(M_A/M_B) \mathbf{r}_{\pi A}] \Phi_B^*(X) v(\mathbf{r}_i - \mathbf{r}_{\pi A}) \Phi_A(X) \chi_i^{(+)} [\mathbf{r}_{\pi A}] dX d^3 r_{\pi A}, \quad (2)$$

$j_i$  is the initial nuclear spin,  $[j_i] = 2j_i + 1$ ,  $A$  denotes the target nucleus,  $B$  denotes the hypernucleus, the  $\omega_\alpha$  are total energies in the meson-nucleus center-of-mass system,  $S^{1/2}$  is the total meson-nucleus center-of-mass energy, and  $X$  is the set of internal baryon coordinates. In obtaining Eq. (2) it was assumed that the kaon is created at the same point that the pion disappears. The distorted waves,  $\chi$ , were obtained from local potentials which were generated<sup>6</sup> by folding the elastic  $t$

matrices of Martin<sup>7</sup> and Davies,<sup>8</sup>

$$U(r) = (2\pi)^{-3} \int \rho(\mathbf{q}) t(\mathbf{q}) \exp(i\mathbf{q} \cdot \mathbf{r}) d^3 q. \quad (3)$$

The results of elastic calculations are shown in Fig. 1 as compared with the data of Marlow *et al.*<sup>9,10</sup> The transition operator in Eq. (2) is taken as the elementary  $t$  matrix from the partial-wave analysis of  $\pi^- + p \rightarrow K^0 + \Lambda$  by Wagner and Lovelace.<sup>11</sup> The elementary

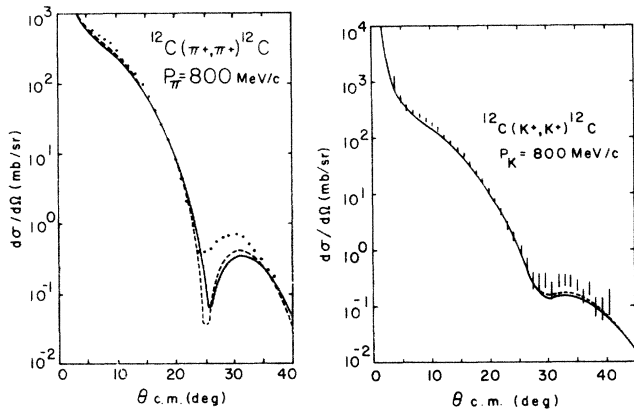


FIG. 1. Comparison of calculated elastic cross sections with the data of Refs. 9 and 10. Solid line is without Fermi averaging of elementary amplitudes; dashed line is with Fermi averaging.

amplitudes are averaged over the momentum distribution of the struck nucleon.

Above lambda threshold the double-differential cross section is given by<sup>12</sup>

$$\frac{d^2\sigma}{d\Omega dE} = (2\pi\hbar^2)^{-1} \sum_{c, J_B} \frac{\mu_c}{k_c} \frac{d\sigma_{cJ_B}}{d\Omega}, \quad (4)$$

where  $\mu_c$  is the lambda reduced mass,  $k_c$  is the  $\Lambda$  asymptotic relative momentum in channel  $c$ ,  $d\sigma_{cJ_B}/d\Omega$  is a fictitious distorted-wave cross section in the form of Eq. (1), calculated for lambda wave functions with flux  $v_c$  in channel  $c$ . The index  $c$  stands for  $\alpha J_c j l$  with  $J_c$  and  $j$  coupled to  $J_B$ , where  $J_c$  is the angular momentum of a possible core state,  $l$  and  $j$  are the lambda orbital and total angular momentum, and  $\alpha$  represents other quantum numbers which are necessary to distinguish core states. Because the sum in Eq. (4) is over all possible ways for the lambda to exit from the nucleus, scattering from resonances and quasifree scattering are included in the calculation.

The structure of  ${}^{12}_\Lambda\text{C}$  is calculated as in Ref. 6 with the interaction of Halderson and Ning.<sup>13</sup> This interaction includes central, spin-spin, symmetric spin-orbit, and tensor components. The core states of  ${}^{11}\text{C}$ , which were included in the calculation, are  $(\frac{3}{2})^-_1$  (0.0),  $\frac{1}{2}^-$  (2.0),  $\frac{5}{2}^-$  (4.319), and  $(\frac{3}{2})^-_2$  (4.804). The wave functions used to describe the states of  ${}^{11}\text{C}$  and  ${}^{12}\text{C}$  are those of Cohen and Kurath.<sup>14</sup> The resulting  ${}^{12}_\Lambda\text{C}$  states provided very good fits to existing  ${}^{12}\text{C}(K^-, \pi^-){}^{12}_\Lambda\text{C}$  data.<sup>6</sup>

The calculations described above are compared in Fig. 2 with the experimental spectra (histogram) of Ref. 2. The normalization of the data was determined from the extractions of peak strengths presented in Ref. 2. The calculation (long-dashed line) has been

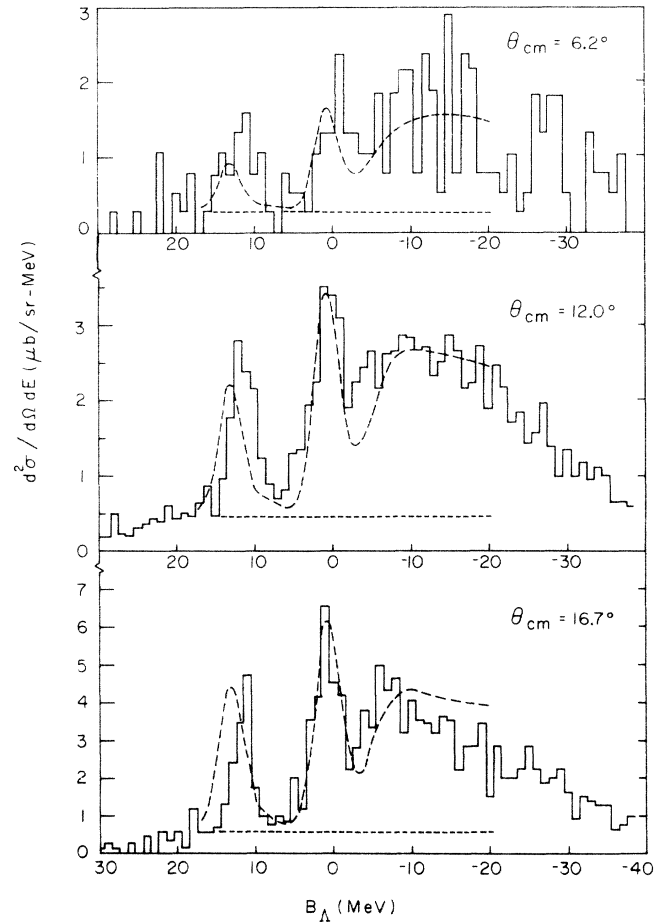


FIG. 2. Comparison of the data of Ref. 2 (histogram) with the calculation (long-dashed line). The calculation has been folded with a Gaussian of width 3.5 MeV and has been multiplied by 3.8. The short-dashed line is the assumed background which was added to the calculation.

folded with a Gaussian of width 3.5 MeV to simulate detector resolution. Comparison with the data should apparently be made only for  $B_\Lambda > -15$  MeV as the spectrometer acceptance becomes limited above that energy.<sup>2</sup> The calculation clearly displays the features of the data, with the ground-state and 11-MeV peaks plus the large quasifree region. Two discrepancies distinguish data from calculations. First, the calculated ground-state peak is  $\sim 2$  MeV low. This is thought to be due to the neglect of the three-body  $\Lambda N N$  interaction. Second, the calculation has been multiplied by a factor of 3.8 in Fig. 2. The need for this factor may be in part accounted for by the 30% normalization uncertainty in the data, but its most probable cause is the choice of elastic potential. The choice used in this paper is very similar to that employed by Ludeking and Walker<sup>1</sup> for their  $(\pi^+, K^+)$  calculations, and produces pure particle-hole cross sections almost identical to

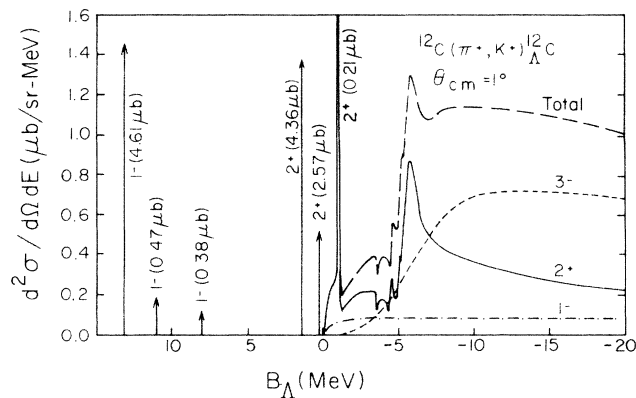


FIG. 3. The calculated  $1^\circ$  double-differential cross section. Above  $\Lambda$  threshold the solid line is  $2^+$  strength, short-dashed line is  $3^-$  strength, dot-dashed line is  $1^-$  strength, and long-dashed line is the sum.

those of Ref. 1. These impulse-approximation potentials differ considerably from best-fit potentials.<sup>9,10</sup> In fact, reasonable fits to ground-state and 11-MeV peaks were obtained in Ref. 2 by use of best-fit elastic potentials.

The theoretical prediction in Fig. 2 can now be dissected to show the spin-parity contributions. This analysis is demonstrated in Fig. 3 where the  $1^\circ$  theoretical spectrum is shown with no folding. States below  $\Lambda$  threshold are shown as vertical arrows. The solid line is the  $2^+$  contribution above threshold, the short-dashed curve is the  $3^-$  contribution, the dot-dashed curve is the  $1^-$  contribution, and the long-dashed curve is the sum of all contributions.

In Fig. 3 one can see the bound  $1^-$  (13.22) and  $1^-$  (11.05) states which comprise the ground-state peak in the data. The excited-state peak in the data, as suggested in Ref. 2, is found to be composed of two bound  $2^+$  states and one narrow  $2^+$  resonance. The main contributor to the quasifree region is from  $3^-$  strength. The dominant configurations of underlying  $3^-$  levels are  $|(\frac{3}{2})_1^- \otimes d_{3/2}(\Lambda)\rangle$  and  $|(\frac{3}{2})_1^- \otimes d_{5/2}(\Lambda)\rangle$ . The lambda escape widths of these levels are 15–18 MeV. This, of course, produces the featureless  $3^-$  spectrum seen in Fig. 3.

The  $2^+$  contribution to the quasifree region does show some structure. Four underlying levels contribute to this structure. The levels are combinations of the  $|(\frac{3}{2})_2 \otimes p_{1/2}\rangle$ ,  $|(\frac{3}{2})_2 \otimes p_{3/2}\rangle$ ,  $|\frac{5}{2} \otimes p_{1/2}\rangle$ , and  $|\frac{5}{2} \otimes p_{3/2}\rangle$  configurations. The one dominant structure is that in which large components of  $|(\frac{3}{2})_2 \otimes p_{1/2}\rangle$  and  $|(\frac{3}{2})_2 \otimes p_{3/2}\rangle$  add in phase. When the calculated spectrum is folded with the 3.5-MeV Gaussian it is seen that this dominant structure is too weak to be identified with the resolution of Ref. 2. This indicates that the structure seen in the data near

$B_\Lambda = -7$  MeV is likely to be statistical. Better-resolution experiments should be able to locate this  $2^+$  strength and its splitting from the  $2^+_2$  state could be used as an additional constraint on the  $\Lambda N$  interaction.

In conclusion, this paper has presented the results of a calculation of  $^{12}\text{C}(\pi^+, K^+)^{12}\text{C}_\Lambda$  in the RCCSM formalism. The calculated cross-section shapes agree very well with the recent data set of Milner *et al.*<sup>2</sup> The features of the data have been identified with the underlying shell-model configurations. The calculated ground-state peak is composed of two  $1^-$  states. The excited-state peak was primarily composed of two bound  $2^+$  states and one  $2^+$  resonance. The quasifree region is primarily a broad distribution of  $3^-$  strength with some contribution from excited  $2^+$  resonances. This calculation has demonstrated comprehensive calculations of hypernuclear formation in the RCCSM approach. It includes bound states, resonances, and quasifree scattering in one coherent framework.

We would like to express our appreciation to Dr. D. Kurath for his assistance in implementing the wave function of Ref. 14, and to Dr. R. J. Philpott for his assistance in extracting continuum wave functions. This work was supported in part by a grant from Research Corporation and by the National Science Foundation under Grant No. PHY-8317084.

(a)Present address: Physics Department, Ohio State University, Columbus, OH 43210.

(b)Present address: Nankai University, Tianjin, China.

<sup>1</sup>C. B. Dover, G. E. Walker, and L. Ludeking, Phys. Rev. C **22**, 2073 (1980); L. Ludeking and G. E. Walker, in Proceedings of the LAMPF Workshop on Nuclear Structure with Intermediate Energy Probes, Los Alamos National Laboratory Report No. LA-8303-C, 1980 (unpublished), p. 286.

<sup>2</sup>C. Milner *et al.*, Phys. Rev. Lett. **54**, 1237 (1985).

<sup>3</sup>D. J. Millener, A. Gal, C. B. Dover, and R. H. Dalitz, Phys. Rev. C **31**, 499 (1986).

<sup>4</sup>R. H. Dalitz and A. Gal, Phys. Lett. **64B**, 154 (1976).

<sup>5</sup>D. Halderson, Phys. Rev. C **30**, 941 (1984).

<sup>6</sup>D. Halderson, P. Ning, and R. J. Philpott, Nucl. Phys. (to be published).

<sup>7</sup>B. R. Martin, Nucl. Phys. **B94**, 413 (1975).

<sup>8</sup>A. T. Davies, Nucl. Phys. **B21**, 359 (1970).

<sup>9</sup>D. Marlow *et al.*, Phys. Rev. C **30**, 1662 (1984).

<sup>10</sup>D. Marlow *et al.*, Phys. Rev. C **25**, 2619 (1982).

<sup>11</sup>F. Wagner and C. Lovelace, Nucl. Phys. **B25**, 411 (1971).

<sup>12</sup>D. Halderson, R. J. Philpott, J. A. Carr, and F. Petrovich, Phys. Rev. C **24**, 1095 (1981).

<sup>13</sup>D. Halderson and P. Ning, Nucl. Phys. **A450**, 391c (1986).

<sup>14</sup>S. Cohen and D. Kurath, Nucl. Phys. **73**, 1 (1965).